Nuclear Instruments and Methods in Physics Research A 1059 (2024) 168951

Contents lists available at ScienceDirect

Nuclear Inst. and Methods in Physics Research, A

journal homepage: www.elsevier.com/locate/nima

Full Length Article

Investigating the possibility of leakage detection in water distribution networks using cosmic ray neutrons in the thermal region

L. Sostero [a,b], D. Pagano [a,b,*], I. Bodini [a,b], G. Bonomi [a,b], A. Donzella [a,b], D. Paderno [a,b], C. Pasini [a], V. Villa [a,b], A. Zenoni [a,b]

[a] Department of Mechanical and Industrial Engineering, University of Brescia, Italy
[b] Istituto Nazionale di Fisica Nucleare (INFN), Pavia, Italy

ARTICLE INFO

Keywords:
Cosmic ray neutrons
CRNS
Water leakages
Thermal neutrons

ABSTRACT

Water distribution systems can experience high levels of leakage, originating from different sources, such as deterioration due to aging of pipes and fittings, material defects, and corrosion. In addition to causing financial losses and supply problems, leakages in treated water distribution also represent a risk for public health. Despite several techniques for leak detection are already available, there is still a lot of interest in new non-invasive approaches, especially for scenarios where acoustic techniques struggle, such as in noisy environmental conditions.

In this work we investigated the possibility of using cosmic ray (CR) neutrons for the detection of underground leakages in water distribution networks, by exploiting the difference in the above ground thermal neutron flux between dry and wet soil conditions. The potential of the technique has been assessed by means of an extensive set of Monte Carlo simulations based on GEANT4, involving realistic scenarios based on the Italian aqueduct design guidelines. Simulation studies focused on sandy soils and results suggest that a significative signal, associated with a leakage, could be detected with a data-taking lasting from a few minutes to a half-hour, depending on the environmental soil moisture, the leaking water distribution in soil, and the soil chemical composition.

Finally, a brief description of a new portable and low-cost detector for thermal neutrons, currently under commission, is also presented.

1. Introduction

Nowadays, modern cities rely on large and complex pipeline networks, providing essential services such as water and sewage distribution. Leakages in distribution networks represent ~80% of the total water loss, with a typical leak wasting between 500 and 1000 times the average consumption of a domestic property [1]. Recent studies estimate the global volume of Non-Revenue Water (NRW) – the amount of water that cannot be billed – at hundreds of billions of cubic meter per year, corresponding to a financial loss of tens of billions of USD per year [2,3]. Leakages along pipelines not only produce financial losses, but also supply problems: some models suggest that by 2050 more than 50% of the global population will suffer from water scarcity at least one month each year [4]. Moreover, water leakages represent a risk for public health – pollutants can contaminate drinkable water through leaks [5,6] – as well as for structures, because of the sinkholes which can occur in the presence of long-term water leaks in quickly dissolving materials [7,8]. Given the importance of the detection of underground leakages, several techniques have been proposed and developed over the years. In this work, we investigated the possibility of using the detection of cosmic ray (CR) induced neutrons in the thermal region as a non-invasive approach to identify underground leakages in water distribution networks.

In the next Section an overview of the current state-of-the-art of leakage detection techniques is given.

2. Overview of the state-of-the-art leakages detection techniques

In general, the localization of the leakage starts with the identification of the leaking pipe. The suspected branch of the network is firstly isolated from the system to have only one source of supply, where a flow meter is installed. Main pipe sections are progressively closed, starting from the farthest segment from the flow meter, cutting off secondary pipes that branch out from the closed sections. An anomalously large change in the measured flow between two successive

* Corresponding author at: Department of Mechanical and Industrial Engineering, University of Brescia, Italy.
E-mail address: davide.pagano@unibs.it (D. Pagano).

https://doi.org/10.1016/j.nima.2023.168951
Received 3 August 2023; Received in revised form 31 October 2023; Accepted 19 November 2023
Available online 29 November 2023

valve closures indicates a leak in the section of pipe that was last shut off [9,10].

Once a coarse localization of the leakage is obtained, its precise position can be assessed by means of several techniques, generally categorized as *acoustic* and *non-acoustic* methods [9]. The leakage of water from a crack in a pipe generates acoustic signals, and by using either aquaphones in direct contact with control valves or ground microphones above the pipe, it is possible to localize the leakage: the stronger the intensity of the signal, the closer the position of the leakage is to the device [11,12]. A more refined technique, which does not require multiple measurements along a pipe, is the *noise correlator*, which is based on the cross-correlation method: from the measurement of the leak noise at just two locations on a pipe, the position of the leak is determined by the time shift of the maximum correlation of the two acoustic signals and the distance between the measurements [13,14].

While acoustic techniques are generally quite good in many cases, they tend to struggle in detecting leaks in low-pressure and/or non-metallic pipes, as well as in noisy environmental conditions. In these scenarios, non-acoustic techniques are generally more suitable. In the past, a common method was based on the use of a tracing: an inert gas (such as a mixture of hydrogen and nitrogen, or helium) was injected into the pipeline, and it was traced as it came out of solution at the leak point [9,15]. Nowadays, instead, the use of Ground Penetrating Radar (GPR) has become much more popular. GPRs scan the subsurface from the ground, by sending high frequency electromagnetic pulses and analyzing the reflection waves. Their working principle is based on the change of the dielectric properties of soil, as a function of its water content [14,16,17].

Other non-acoustic approaches, investigated in literature, include techniques based on thermography and the use of time-domain reflectometers (TDRs). The former are based on the difference in temperature between the ground soil above a leak and areas further away from it, which is measured by means of thermal infrared radiation [15]. Recently, this technique has also been employed for the detection of leakages in district heating networks by means of remote sensing from an aircraft with a thermal camera [18]. The use of time-domain reflectometers has recently gained popularity, as it allows an online monitoring of pipelines and the localization of water leaks. TDRs measure variations of the dielectric characteristics of a propagation line, in contact with the pipeline, which originate from the presence of leaks [19,20]. While this technique has been proven to be very effective, it requires sensing elements to be buried along the pipe at the time of installation, strongly limiting its field of application.

As suggested by the large number of techniques currently used for the detection of leakages, at present it does not exist a unique approach which works for all scenarios. In this work, we present an alternative low-invasive technique for the detection of underground leakages, based on the use of cosmic ray neutrons in the thermal region.

3. The method

The interactions of primary cosmic rays with the upper layers of the atmosphere generate air showers through nuclear reactions and high-energy neutrons (~100 MeV) are produced among many other high energy particles [21–23]. In addition to this *ultrafast* component, lower energy neutrons, with energy of $O(1)$ MeV, are also released by the evaporation of excited nuclei that interacted with high-energy nucleons [24]. When traveling through the atmosphere, *fast* neutrons, at MeV energy scale, slow down to *epithermal* and *thermal* energies (0.025 eV at 20 °C), by means of collision with other nuclei. This process of moderation is more effective for neutrons interacting with light nuclei and, in particular, with hydrogen nuclei.

When CR neutrons reach the ground, they penetrate the soil, where they can be further moderated. Neutrons may diffuse back from soil to air (*albedo* neutrons), and their intensity above the surface is correlated with the soil composition and moisture: the larger the hydrogen content in soil, the larger the reduction of fast and epithermal neutrons in the albedo flux, as an increasing fraction of them are moderated to thermal energy [25]. Of course, the concentration of hydrogen in the soil is strongly correlated to its water content.

Cosmic Ray Neutron Sensing (CRNS) is a technique developed more than ten years ago for above ground monitoring of the soil moisture and environmental humidity, in favor of climate science, agriculture and hydrological models at field scale [25,26]. The technique is based on the rather complex dependence of the epithermal cosmic ray neutron flux above ground on the environmental hydrogen content [27].

Nowadays, CRNS has been successfully used in agriculture to measure the environmental water content, in the most superficial layers of soil, in a footprint area with a radius of more than 200 m, by using detectors for epithermal neutrons, placed at a small distance from the ground [24,28,29]. Due to the complexity of the hydrological processes, an absolute and reliable assessment of the soil water content, from the measurement of the albedo neutron flux, requires the use of very elaborate multivariate models, taking into account the soil composition, many atmospheric parameters, the presence, and type of vegetation, and much more [24].

In a similar fashion, this paper proposes a method to identify water leakages in underground pipelines, exploiting the difference in the above ground thermal neutron flux between dry and wet soil conditions. With respect to CRNS for agricultural applications, here we do not need an absolute assessment of the soil moisture, but instead, we are only interested in localizing underground regions with an anomalous large water content with respect to the surrounding soil. This goal, together with the fact that the position of the pipes in distribution networks is known, suggests the use of relative measurements, so that the approach is completely data-driven. Another difference with the CRNS technique is that the latter relies on the detection of epithermal neutrons, as more abundant and highly sensitive to soil moisture [25]. However, their detection is much more complex than that of thermal neutrons, requiring either expensive detectors or thermal detectors surrounded by properly sized moderating materials. For this reason, we decided to investigate the potential of the proposed technique with thermal neutrons.

To investigate the potential of the technique, a set of Monte Carlo simulations, based on GEANT4 version 4.11.01, was performed. GEANT4 [30] is a toolkit for the simulation of the passage of particles through matter, whose field of applications is very wide: from high energy physics at colliders [31] to medical and biological physics [32]. Moreover, GEANT4 supports low energy neutron transport, which is relevant for our studies, via the Neutron High-Precision package, which is continuously updated in response to the growing interest in neutron propagation simulations [33].

The geometry modeled in GEANT4 is shown in Fig. 1 and represents a buried water pipe with a leakage localized in its top part. Dimension and burial depth have been chosen according to the Italian aqueduct design guidelines [34,35]: the pipe, with a diameter of 200 mm, is made of PVC and is buried at a depth of 900 mm. The surrounding soil consists of 50% in volume of solid material (porosity of 50%), of which 90% in volume is SiO_2 and the remaining 10% is Al_2O_3, that is the typical composition for sandy soil [36]. The soil density amounts to 1.43 g/cm^3, and the pore space of the soil is filled with air and eventually with water leaked from the pipe [37].

The soil moisture distribution around the leakage point, both in shape and water content, is based on recent numerical and experimental studies on water propagation from a leakage [38]. The authors considered a porous soil with high permeability coefficient, such as sandy and silt soils, and we appropriately scaled their model to this case study. Above the soil surface, a detector of thermal neutrons, described in the next Section, is horizontally placed a few cm from the ground. Cosmic neutrons are generated from a planar source at 2.5 m from ground, using the EcoMug generator, a tool intended for the generation

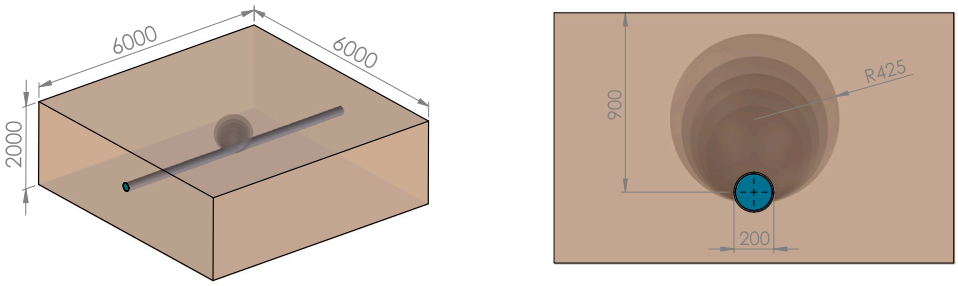

Fig. 1. Pipe with a leakage as modeled in GEANT4 (lengths in mm). The soil moisture distribution around the pipe has been modeled according to literature [38]. It varies from 50% near the leaking point to 10% far from it, as represented by the shades of brown of the concentric spheres.

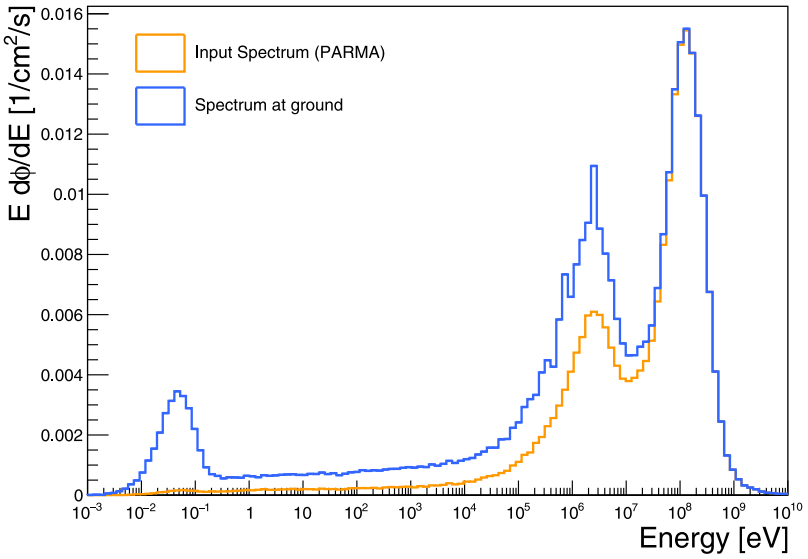

Fig. 2. Differential flux as a function of the neutron energy. The orange line denotes the input flux in the simulations, as obtained from the PARMA model, whereas the blue line indicates the flux measured at the detector position, which also includes the albedo component.

of muons that can be easily adapted to any kind of particle, neutrons included [39].

The differential flux of cosmic neutrons comes from the PARMA analytical model, which estimates the cosmic ray fluxes (neutrons, but also muons, electrons, etc.) as a function of the geographic coordinates and altitude [40,41]. For our simulations, the spectrum refers to the coordinates of Rome at ground level (0 m altitude). The input spectrum is indicated by the orange line in Fig. 2, whereas the energy spectrum at the level of the detector is also reported as a blue line. As expected, the interaction with the soil (water content of 10% in this case) moderates $O(1)$ MeV cosmic neutrons down to lower energies, and an epithermal shoulder with a thermal peak arises.

4. Results

For thermal neutrons, an efficient and cost-effective solution is to use a detector exploiting the nuclear reaction ^{6}Li(n-α)^{3}H, such as the EJ-426HD-PE2 from Eljen Technology, which is also what we chose for our detector, described in Section 5. Its efficiency as a function of the neutron energy has been estimated by knowing the cross section of the ^{6}Li(n-α)^{3}H reaction, from the CENDL 3.2 library [42], and the ^{6}Li density of the scintillating material. The result is shown in Fig. 3.

As mentioned before, the idea is to measure how the relative rate of the thermal neutrons changes as moving a detector along the pipe under investigation. The detector simulated in our studies consists of a sensitive layer, with area 30 × 30 cm^2, enclosed in a polylactic acid (PLA) case, with a thickness ranging from 1.2 mm to 2.2 mm. These

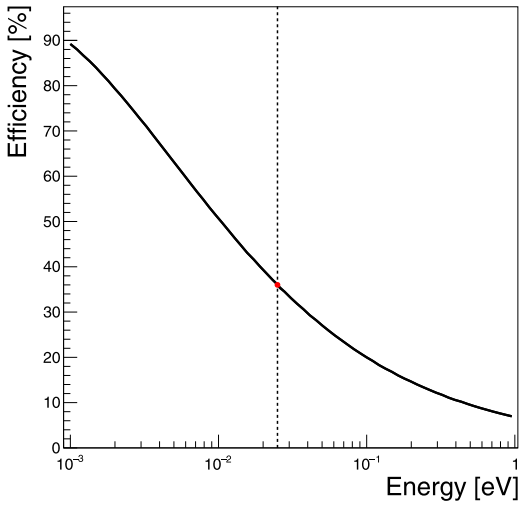

Fig. 3. Estimated efficiency for the EJ-426HD-PE2 detector as a function of the energy. The dotted line indicates the energy value of 0.025 eV, which corresponds to an estimated efficiency of ~36%.

specifications follow the design of the detector COMMAND, described in Section 5.

We then simulated the number of detected neutrons along the pipe, taking into account the estimated efficiency of the EJ-426HD-PE2 as

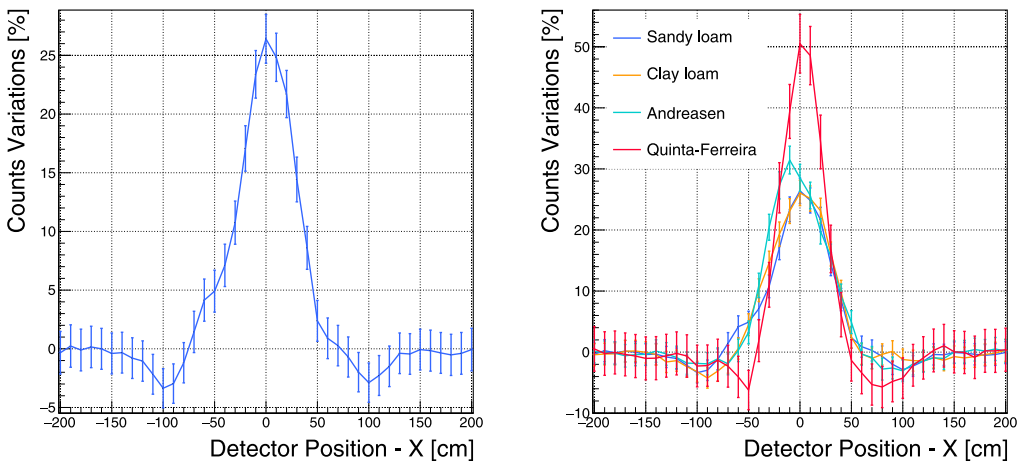

Fig. 4. (left): Relative variation of detected neutrons for a benchmark sandy soil in dry condition, as described in the text. (right): Relative variation of detected neutrons for four different soil compositions as described in the text. Error bars are statistical only and correspond to one standard deviation.

a function of the energy, by moving the detector by steps of 10 cm. For each measurement, the generated statistics corresponded to a data taking of ∼30 min. Fig. 4-left shows the first results for the benchmark sandy soil in dry condition, that is with a uniform soil moisture of 2%. The leakage point is localized at $x = 0$ and the y-axis represents the relative variation of detected neutrons with respect to what would be measured, at the same position, without the leakage. As it can be noticed, the maximum relative variation of counts is localized in correspondence to the leakage and the resulting curve, as a function of the detector position, has a full width half maximum of ∼50 cm, which makes it possible a good localization of the crack along the pipe.

While previous results are encouraging, they are based on an over-simplified model when it comes to the soil composition and its moisture. Indeed, the main parameters which can impact the performance of the technique are the chemical composition of soil, the initial soil moisture (that is, in absence of leakage), and the leaked water distribution around the pipe. In the following, all these parameters are discussed and evaluated with dedicated simulations. Finally, Section 4.4 also discusses how the acquisition time impacts on the expected significance of the signal.

4.1. Impact of soil composition

The chemical composition of the soil may have a strong impact on thermal neutrons, as their flux may be reduced by the presence of elements with a high absorption cross section. For this reason, in addition to the sandy soil, we also evaluated a clay soil (75% SiO_2, 25% Al_2O_3), and other two compositions from Quinta-Ferreira et al. [43] and Andreasen et al. [44], which are based on X-ray Fluorescence analyses on real samples of soils. In addition to SiO_2 and Al_2O_3, these two soils also include varying amounts of P, K, Ca, Ti, and Fe. Additionally, traces of Cl, Mn, and Cd, are reported by Quinta-Ferreira et al. whereas Andreasen et al. measured the presence of few ppm of Gd. All these elements have a large absorption cross section to thermal neutrons.

To isolate the impact of soil composition, we proceeded by using the same soil moisture and the same model for the water leakage propagation described before. The latter is of course an approximation, since the soil moisture distribution around the leakage comes from literature studies on soils with high porosity and hydraulic conductivity, as sandy loam. Fig. 4-right shows the result. Although no difference between sandy and clay loam are observed, the presence of absorbing elements results in a larger relative variation of counts. Indeed, the distance thermal neutrons have to travel to reach the detector is on average longer in the absence of leakage, as epithermal neutrons tend to be thermalized at deeper depths, because of the lower content of water.

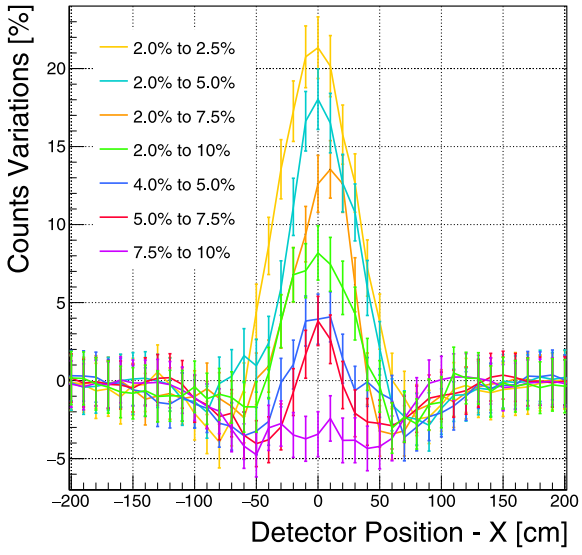

Fig. 5. Percent counts variations of detected neutrons along the leaking pipe on a sandy loam with a linear gradient on the environmental moisture. Error bars are statistical only and correspond to one standard deviation.

Thanks to this, while the presence of absorbing elements reduces the overall statistics of detected thermal neutrons (as the larger statistical error bars in Fig. 4-right indicate), its impact is larger in the absence of leakages and this increases the expected signal.

4.2. Impact of soil moisture

The environmental water content in soil has the largest impact on the performance of the proposed method. Indeed, the higher the initial content of water is, the lower is the expected signal, as the overall increase of water in the soil makes the local excess of moisture around the leakages less significative. For sandy soils, typical moisture may vary from 2% to 10%, the latter being the wettest drained state [45]. Near-surface layers are typically drier than the ones at lower depths, therefore we considered a linear gradient for the moisture in our simulations. Fig. 5 shows the results for several scenarios of moisture, using a sandy soil and the same model for the leaked water distribution reported in Fig. 1.

Minimum and maximum values of moisture are reported in the legend of the plot. In all cases, the maximum value is reached at a

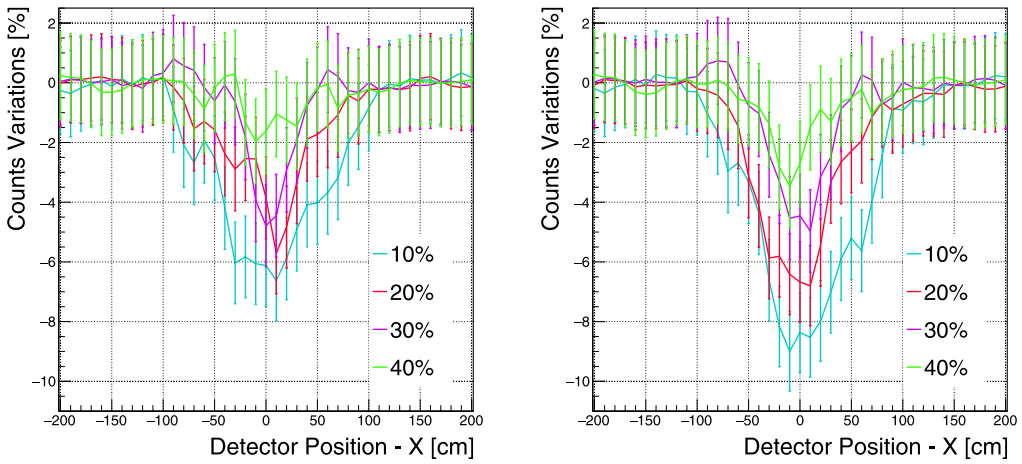

Fig. 6. Percent counts variations of detected neutrons along the leaking pipe on a sandy loam with a uniform initial soil moisture. The plot on the left is produced with the benchmark model for the leaked water distribution, described in the text, whereas the plot on the right corresponds to the same model but with a 50% increase of the overall water content. Error bars are statistical only and correspond to one standard deviation.

depth of 75 cm and is kept constant for all the soil below. As expected, increasing the environmental soil moisture leads to a reduction in the signal variation. The comparison between the 2.0%-to −10% and 7.5%-to −10% curves also suggests that what drives the results is the water content near the surface, something which has already been discussed in literature [24,46].

Fig. 6-left shows the results for even wetter initial conditions, with a uniform soil moisture ranging from 10% to 40%. In these cases, the increase of neutrons thermalized at high depth, due to the leaked water, is counterbalanced by the increase of the absorption cross-section of the soil, due to the higher hydrogen content [47]. Because of this, thermal neutrons far from the surface are more likely to be absorbed before reaching the surface, resulting in a negative counts variation. Of course, the effect tends to be less significative as the soil moisture increases, as the relative change of the water content nearby the leakage is smaller for a soil in already wet conditions.

For soils such as clay loam, it must be considered that the low hydraulic conductivity not only tends to increase the environmental soil moisture, but also the local variation of the water content nearby the leakage, because of the slow drainage. These two effects go in different directions for what concerns the expected signal. As an example, Fig. 6-right has been produced in the same conditions as in Fig. 6-left, but with a 50% increase of the overall water content in the leakage model. In all curves, the negative peak associated to the leakage is enhanced.

4.3. Impact of leaked water distribution

Size and shape of leaked water from a pipe, in the soil, depends on several parameters, such as pipe pressure, crack size, its position, and so on. Moreover, size and shape also evolve over time. In order to evaluate how these parameters may affect the performance, we considered two additional models of leaked water distribution. The first one has half of the volume of the one shown in Fig. 1, but with the same shape. The second one has, instead, a similar volume, but a different shape, as originated from a lateral crack on the pipe, as modeled in [38]. Results from all three considered models are shown in Fig. 7-left: Case #1 in the label refers to the original model of Fig. 1, Case #2 refers to the model with half volume, whereas Case #3 refers to the one originated from the lateral crack. All simulations are based on the benchmark sandy loam with uniform 2% of initial soil moisture.

While the reduction of the expected signal for Case #2, that is when considering a model with only 50% of the original volume of leaked water, is expected, the large reduction for Case #3 is less trivial and needs a comment. In this case, indeed, the pressured water horizontally flowing out of the crack generates a high moisture distribution which has two major differences with respect to the one in Case #1: (i) it is at lower depth (on average); (ii) its center is displaced by few tens of centimeters with respect to the pipe direction. Both effects go in the direction of reducing the signal. However, by moving the detector closer to the center of the distribution, a large fraction of the signal lost with respect to Case #1 can be recovered. This suggests the possibility of completing the scan along the pipe direction with measurements around the region in which a peak is eventually identified. Indeed, while the count variation at $x = 0$ is small in absolute terms, the peak is still identifiable when moving along the pipe, as the red curve indicates.

4.4. Impact of acquisition time

As a last step in characterizing the potential of the proposed technique, we assessed how the expected significance of the signal changes as a function of the acquisition time and for several of the scenarios considered in this work.

The results are shown in Fig. 8, where the significance is measured in Gaussian standard deviations σ. Although the Figure does not include systematic effects related to the measurement, which will be assessed once the detector described in Section 5 is finalized, it gives a feedback on the possibilities of identifying the leakage for the following cases: (i) sandy soil with 2% uniform moisture (yellow); (ii) same as (i), but with a 50% volume reduction of leaked water (red); (iii) sandy soil with a linear gradient of moisture from 2% to 10% (cyan); (iv) same as (i), but with the leakage originating from the side of the pipe (purple).

For each case, the significance versus acquisition time appears as a band as we additionally take into account the possible displacement in the direction of the pipe, from 0 (topmost line) to 20 cm (bottommost line), between the detector and center of the leaked water distribution. For the case associated to the lateral crack on the pipe, this additional displacement goes, of course, in the direction of further pushing away the detector from the leak. Results suggest that, in most of the cases here presented, a data-taking of a few minutes could be enough to identify the presence of the leakage. On the other hand, the purple band also suggest the importance of additional measurements around the region of the peak, to reduce the distance between the detector and the core of leakage water.

Although simulations provided encouraging results, experimental measurements are necessary and therefore, with this goal, we designed and developed a low-cost suitable detector – called COMMAND (COMpact Muon And Neutron Detector) – which is described in the next Section.

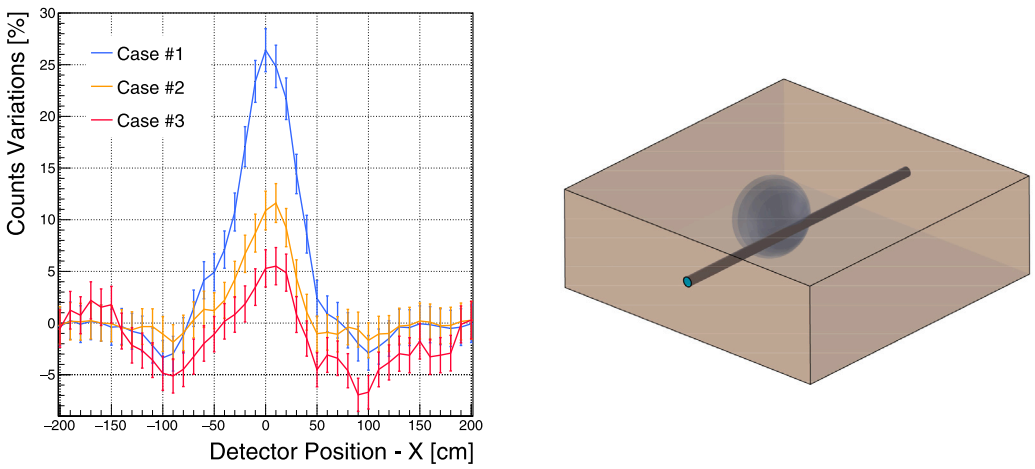

Fig. 7. (left): Percent counts variations of detected neutrons along the leaking pipe on a sandy loam in dry conditions with a leakage as the one presented Fig. 1 (Case #1), with a 50% in volume smaller one (Case #2), and with a leakage originating from an orifice on the side of the pipe (Case #3). Error bars are statistical only and correspond to one standard deviation. (right) Leakage originating from the side of the pipe as modeled in GEANT4.

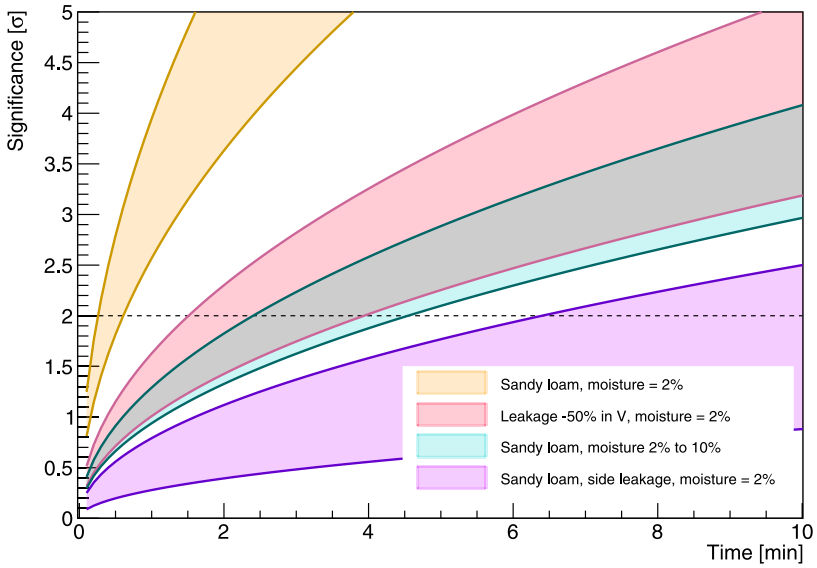

Fig. 8. Significance of the signal, measured in Gaussian standard deviations, as a function of the data taking time and for several scenarios as described in the text. For each scenario, the curves are displayed as bands to also take into account the possible displacement in the direction of the pipe, from 0 (topmost line) to 20 cm (bottommost line), between the detector and center of the leaked water distribution, as explained in the text.

5. The COMMAND detector

Results from previous simulation studies led us to design and develop a low-cost detector, suitable for the identification of underground leakages. For the detection of thermal neutrons, we chose the EJ-426HD-PE2 from Eljen Technology, which is a thin sheet consisting of particles of lithium-6-fluoride (^{6}Li) and zinc sulfide phosphor (ZnS:Ag), dispersed in a binder. The neutron detection process is based on the nuclear reaction ^{6}Li(n, α)^{3}H – with a cross section of 941 barns for 0.025 eV neutrons – where the resulting triton and alpha particles are detected by the ZnS:Ag, emitting a broad blue scintillating light. The choice of EJ-426HD-PE2 was driven by its affordable cost (compared to alternatives based on ^{3}He and ^{10}B) and good conversion efficiency, which is ∼36%.

The output scintillating light is shifted to green, by means of a wavelength shifter (WLS), and read by an array of silicon photomultipliers (SiPMs). For the WLS we chose the EJ-280 from Eljen Technology, whereas for the SiPMs we opted for ASD-NUV4S-P from AdvanSiD, with a 4×4 mm^2 sensitive area. The choice of the ASD-NUV4S-P was mainly driven by the low noise and excellent temperature stability. The signal from the EJ-426HD-PE2 is read by 4 SiPMs, which are directly mounted on the front-end electronics, as indicated by numbers from 1 to 4 in Fig. 9-left. The front-end electronics deals with (in the following order): (i) reading all the signals from the SiPMs; (ii) amplification, which can be independently set for each channel; (iii) discrimination; (iv) sending the analogue signals, after a 16-bit DAC, to the PLC, which deals with the data acquisition.

The EJ-426HD-PE2, the WLS, and the front-end electronics are enclosed in a 3D-printed shell made of PLA, as shown in Fig. 10, which does not significantly impact the response of the detector to thermal neutrons due to its small thickness, that varies from 1.2 mm to 2.2 mm. The light proofing has been obtained with a proper design and the use of neoprene at the openings for the cable passage.

As the proposed strategy for the identification of underground leakages is based on multiple measurements along the pipe, we decided to build two modules for the simultaneous detection of neutrons at different positions along the tube, to speed up the overall data acquisition process. One module is installed in a weather-proof case as the one shown in Fig. 11, which hosts also the PLC and the battery, while the other one is placed in a smaller case, and it is connected to

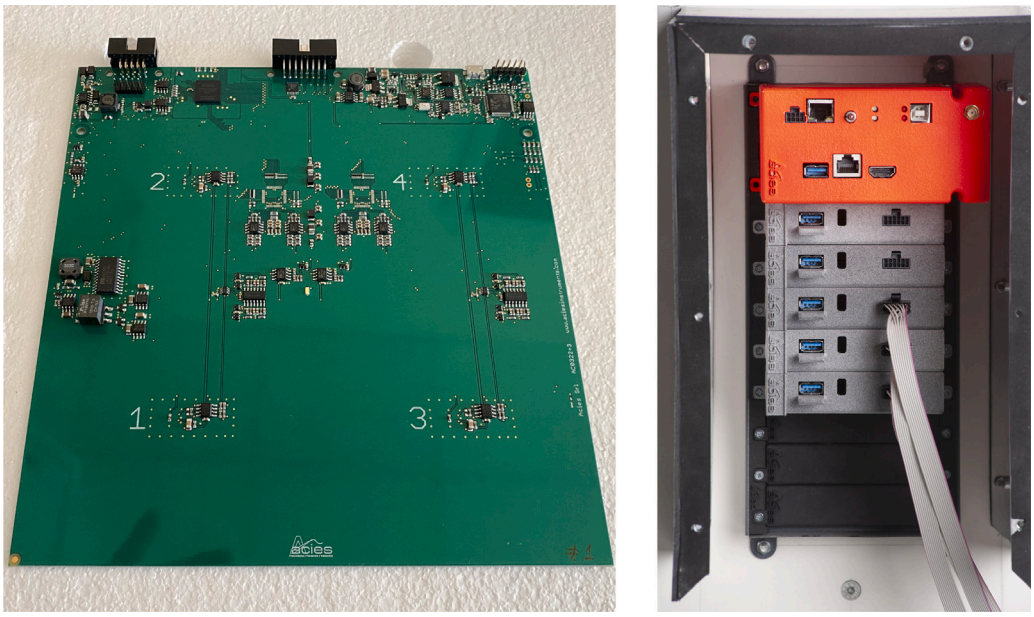

Fig. 9. (left): Front-end electronics each neutron module in COMMAND. (right): PLC for the data acquisition in COMMAND.

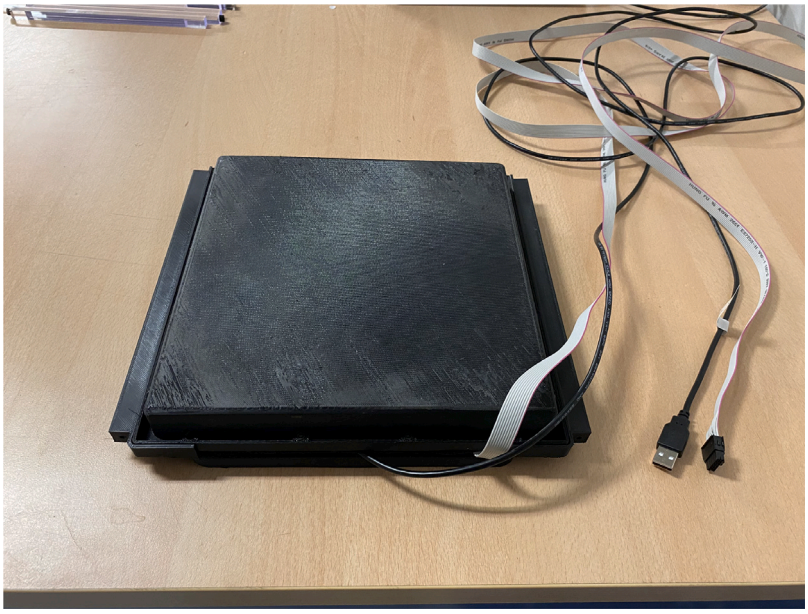

Fig. 10. 3D-printed shell of a neutron module.

the PLC through a flat cable. Both cases are built around aluminum construction profiles and thin panels, which have a negligible impact on the performance of the detector. The large case in Fig. 11, with a size of approximately $33 \times 33 \times 110$ cm^3, is deliberately oversized as it can also house modules for the detection of muons for other applications. The other case, currently under construction, has the same base area but its height is only ∼20 cm. The overall weight of the detector, with all modules but the battery, is ∼15 kg.

As previously mentioned, the two modules for the detection of neutrons are connected to the same PLC and share the data acquisition (DAQ). The PLC was produced by Acies – an Italian manufacturer of analog and digital electronics – and it also handles the supply management. The maximum power consumption is ∼7 W, which is driven by the DAQ. Indeed, the PLC, which is based on a Raspberry with dual-core ARM Cortex processor and 4 GB DDR4-RAM, also handles services such as Wi-Fi, two GPS modules, USB 3.0 protocol, and data storage. The system can run on 100 Ah @ 12 V car battery for approximately one day.

Concerning the cost of the detector, if we only take into account the modules and the front-end electronics dedicated to the detection of neutrons (COMMAND also have three modules dedicated to the detection of muons, which are not relevant for this manuscript), it is approximately equal to 6.5 k€.

The COMMAND detector is almost finalized. All hardware-related activities (electronics, mechanical supports, etc.) are completed, and the work is now focused on finalizing the software for the DAQ, testing each module, and equalizing all channels by characterizing the SiPMs onboard (breakdown voltage, gain versus overvoltage, etc.). This is a work-in-progress, but preliminary results are encouraging: Fig. 12 shows a candidate neutron signal as recorded by the four SiPMs of a single neutron module. Although at that time one channel was noisier than the others, due to an unoptimized overvoltage, the redundancy of

Fig. 11. View of one of the weather-proof cases for the neutron modules. The PLC, as well as the battery for field measurements, are housed in a removable case anchored to the left side of the main structure, as in the picture on the right.

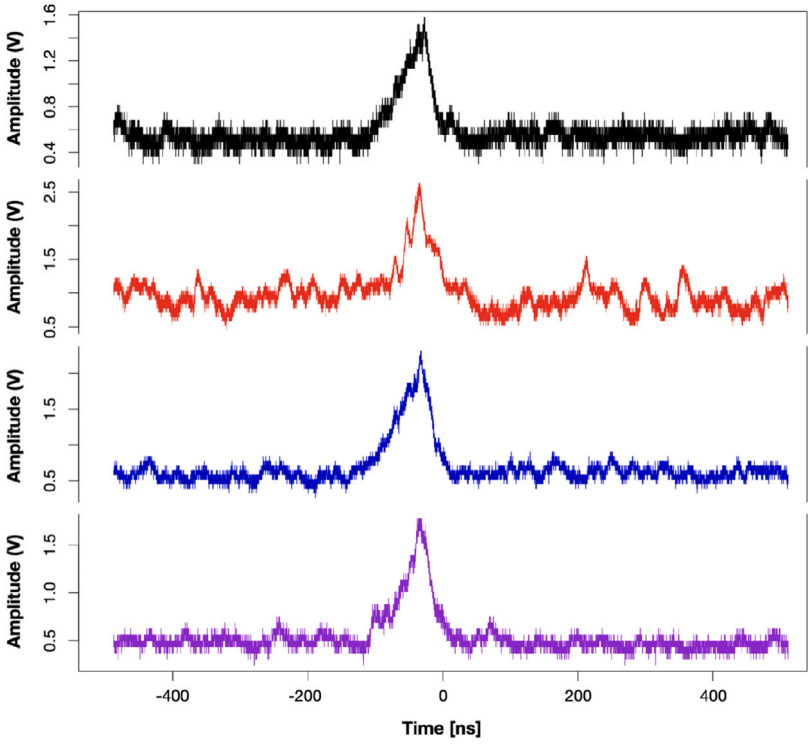

Fig. 12. Candidate neutron signal as recorded by the four SiPMs of a single neutron module.

having four SiPMs opens to different options of triggering, resulting in a high purity signal.

The work on the detector is expected to last few more months and first on-field measurements are expected by the beginning of 2024.

6. Conclusions

This study investigated the possibility of using cosmic ray neutrons for the identification of underground water leakage. As the position of the pipes is known, the proposed technique is based on the measurement of how the relative rate of the thermal neutrons changes as moving a detector along the pipe under investigation.

Extensive MC simulations, based on GEANT4, were performed considering a realistic scenario of leaking pipe in a water distribution network. Geometry (pipe section and depth), materials and compositions, as well as the modeling of the leakage, were based on literature. We also evaluated how the chemical composition of soil, its moisture, as well the size and shape of leaked water distribution impact on the performance of the technique. Results show that the environmental soil moisture has the largest impact on performance.

For fast draining soils, such as sandy soils, the data acquisition time, necessary to collect a statistically significant signal, is expected to range

from a few minutes, for dry initial conditions, to half an hour for the wettest soil conditions.

As mentioned in Section 4.2, for soils with low hydraulic conductivity, such as clay loam, the slow drainage not only tends to increase the environmental soil moisture, but also the local variation of the water content nearby the leakage. These two effects go in different directions for what concerns the expected signal. Simulations indicate that an increase of 50% of the overall water content nearby the leakage results in an enhancement of few percents of the expected signal for large values of the environmental soil moisture.

Encouraging results from the simulation studies led us to design and develop a low-cost detector, suitable for the identification of underground leakages. The proposed detector, called COMMAND, detects thermal neutrons by means of the nuclear reaction ^{6}Li(n, α)^{3}H in a thin sheet consisting of particles of lithium-6-fluoride (^{6}Li) and zinc sulfide phosphor (ZnS:Ag), dispersed in a binder. The scintillating light from the ZnS:Ag is then detected by an array of SiPMs. The detector is at the late stage of development, which is expected to a last few more months, with first on-field measurements expected by the beginning of 2024.

Declaration of competing interest

The authors declare that they have no known competing financial interests or personal relationships that could have appeared to influence the work reported in this paper.

Data availability

No data was used for the research described in the article.

Acknowledgments

The authors acknowledge the support from the University of Brescia, Italy and the National Institute of Nuclear Physics (INFN), Italy. The work of L. Sostero was co-funded by the European Union (Piano Nazionale di Ripresa e Resilienza – Next Generation EU – Decreto Ministeriale 352/2022).

References

[1] D. Rogers, Leaking water networks: An economic and environmental disaster, Procedia Eng. 70 (2014) 1421–1429, http://dx.doi.org/10.1016/j.proeng.2014.02.157.

[2] R. Liemberger, A. Wyatt, Quantifying the global non-revenue water problem, Water Supply 19 (3) (2018) 831–837, http://dx.doi.org/10.2166/ws.2018.129.

[3] R. Vanijjirattikhan, S. Khomsay, N. Kitbutrawat, K. Khomsay, U. Supakchukul, S. Udomsuk, J. Suwatthikul, N. Oumtrakul, K. Anusart, AI-based acoustic leak detection in water distribution systems, Results Eng. 15 (2022) 100557, http://dx.doi.org/10.1016/j.rineng.2022.100557.

[4] World Water Assessment Programme (United Nations), The united nations world water development report 2018, 2018, URL https://www.unwater.org/publications/world-water-development-report-2018/.

[5] C.M. Fontanazza, V. Notaro, V. Puleo, P. Nicolosi, G. Freni, Contaminant intrusion through leaks in water distribution system: Experimental analysis, Procedia Eng. 119 (2015) 426–433, http://dx.doi.org/10.1016/j.proeng.2015.08.904.

[6] L. Ducci, P. Rizzo, R. Pinardi, A. Solfrini, A. Maggiali, M. Pizzati, F. Balsamo, F. Celico, What is the impact of leaky sewers on groundwater contamination in urban semi-confined aquifers? A test study related to fecal matter and personal care products (PCPs), Hydrology 10 (1) (2022) 3, http://dx.doi.org/10.3390/hydrology10010003.

[7] P. Carrive, A. Saintenoy, E. Léger, S.A. Arcone, P. Sailhac, Exploiting ground-penetrating radar signal enhancements by water-saturated bulb surrounding defective waterpipes for leak detection, Geosciences 12 (10) (2022) 368, http://dx.doi.org/10.3390/geosciences12100368.

[8] M.O. Alsaydalani, Effect of orifice hydraulic and geometric characteristics on leakage in water distribution systems, Int. J. Geomate 25 (107) (2023) http://dx.doi.org/10.21660/2023.107.3737.

[9] M. Farley, S. Water, W. Supply, S.C. Council, W.H. Organization, et al., Leakage Management and Control: A Best Practice Training Manual, Tech. Rep., World Health Organization, 2001.

[10] P. Boulos, T. Schade, C.W. Baxter, Locating leaks in water distribution systems using network modeling, J. Water Manage. Model. (2008) http://dx.doi.org/10.14796/jwmm.r228-21.

[11] A.N. Tafuri, Locating leaks with acoustic technology, 92 (7) (2000) 57–66. http://dx.doi.org/10.1002/j.1551-8833.2000.tb08973.x.

[12] S.B. Shimanskii, B.P. Strelkov, A.N. Anan'ev, A.M. Lyubishkin, T. Iijima, H. Mochizuki, Y. Kasai, K. Yokota, J. Kanazawa, Acoustic method of leak detection using high-temperature microphones, At. Energy 98 (2) (2005) 89–96, http://dx.doi.org/10.1007/s10512-005-0175-9.

[13] O. Hunaidi, A. Wang, M. Bracken, T. Gambino, C. Fricke, Acoustic methods for locating leaks in municipal water pipe networks, 2004, URL https://api.semanticscholar.org/CorpusID:17016338.

[14] A.D. Coster, J.P. Medina, M. Nottebaere, K. Alkhalifeh, X. Neyt, J. Vanderdonckt, S. Lambot, Towards an improvement of GPR-based detection of pipes and leaks in water distribution networks, J. Appl. Geophys. 162 (2019) 138–151, http://dx.doi.org/10.1016/j.jappgeo.2019.02.001.

[15] O. Hunaidi, W. Chu, A. Wang, W. Guan, Detecting leaks in plastic pipes, Amer. Water Works Assoc. 92 (2) (2000) 82–94, http://dx.doi.org/10.1002/j.1551-8833.2000.tb08819.x.

[16] W.W. Lai, R.K. Chang, J.F. Sham, K. Pang, Perturbation mapping of water leak in buried water pipes via laboratory validation experiments with high-frequency ground penetrating radar (GPR), Tunn. Undergr. Space Technol. 52 (2016) 157–167, http://dx.doi.org/10.1016/j.tust.2015.10.017.

[17] A. Stampolidis, P. Soupios, F. Vallianatos, G. Tsokas, Detection of leaks in buried plastic water distribution pipes in urban places - a case study, in: Proceedings of the 2nd International Workshop on Advanced Ground Penetrating Radar, 2003, Int. Res. Centre for Telecommunications-Transmission & Radar, http://dx.doi.org/10.1109/agpr.2003.1207303.

[18] O. Friman, P. Follo, J. Ahlberg, S. Sjokvist, Methods for large-scale monitoring of district heating systems using airborne thermography, IEEE Trans. Geosci. Remote Sens. 52 (8) (2014) 5175–5182, http://dx.doi.org/10.1109/tgrs.2013.2287238.

[19] D.A. Robinson, S.B. Jones, J.M. Wraith, D. Or, S.P. Friedman, A review of advances in dielectric and electrical conductivity measurement in soils using time domain reflectometry, Vadose Zone J. 2 (4) (2003) 444–475, http://dx.doi.org/10.2136/vzj2003.4440.

[20] A. Cataldo, E.D. Benedetto, G. Cannazza, G. Monti, C. Demitri, Accuracy improvement in the TDR-based localization of water leaks, Results Phys. 6 (2016) 594–598, http://dx.doi.org/10.1016/j.rinp.2016.08.012.

[21] K. Gudima, S. Mashnik, V. Toneev, Cascade-exciton model of nuclear reactions, Nuclear Phys. A 401 (2) (1983) 329–361, http://dx.doi.org/10.1016/0375-9474(83)90532-8.

[22] D. Desilets, M. Zreda, On scaling cosmogenic nuclide production rates for altitude and latitude using cosmic-ray measurements, Earth Planet. Sci. Lett. 193 (1–2) (2001) 213–225, http://dx.doi.org/10.1016/s0012-821x(01)00477-0.

[23] G. Bonomi, P. Checchia, M. D'Errico, D. Pagano, G. Saracino, Applications of cosmic-ray muons, Prog. Part. Nucl. Phys. 112 (2020) 103768.

[24] M. Köhli, M. Schrön, M. Zreda, U. Schmidt, P. Dietrich, S. Zacharias, Footprint characteristics revised for field-scale soil moisture monitoring with cosmic-ray neutrons, Water Resour. Res. 51 (7) (2015) 5772–5790, http://dx.doi.org/10.1002/2015wr017169.

[25] M. Zreda, D. Desilets, T.P.A. Ferré, R.L. Scott, Measuring soil moisture content non-invasively at intermediate spatial scale using cosmic-ray neutrons, Geophys. Res. Lett. 35 (21) (2008) http://dx.doi.org/10.1029/2008gl035655.

[26] D. Desilets, M. Zreda, T.P.A. Ferré, Nature's neutron probe: Land surface hydrology at an elusive scale with cosmic rays, Water Resour. Res. 46 (11) (2010) http://dx.doi.org/10.1029/2009wr008726.

[27] M. Köhli, J. Weimar, M. Schrön, R. Baatz, U. Schmidt, Soil moisture and air humidity dependence of the above-ground cosmic-ray neutron intensity, Front. Water 2 (2021) http://dx.doi.org/10.3389/frwa.2020.544847.

[28] M. Zreda, W.J. Shuttleworth, X. Zeng, C. Zweck, D. Desilets, T. Franz, R. Rosolem, COSMOS: the COsmic-ray soil moisture observing system, Hydrol. Earth Syst. Sci. 16 (11) (2012) 4079–4099, http://dx.doi.org/10.5194/hess-16-4079-2012.

[29] L. Stevanato, G. Baroni, Y. Cohen, C.L. Fontana, S. Gatto, M. Lunardon, F. Marinello, S. Moretto, L. Morselli, A novel cosmic-ray neutron sensor for soil moisture estimation over large areas, Agriculture 9 (9) (2019) http://dx.doi.org/10.3390/agriculture9090202, URL https://www.mdpi.com/2077-0472/9/9/202.

[30] S. Agostinelli, J. Allison, K. Amako, J. Apostolakis, H. Araujo, P. Arce, M. Asai, D. Axen, S. Banerjee, G. Barrand, F. Behner, L. Bellagamba, J. Boudreau, L. Broglia, A. Brunengo, H. Burkhardt, S. Chauvie, J. Chuma, R. Chytracek, G. Cooperman, G. Cosmo, P. Degtyarenko, A. Dell'Acqua, G. Depaola, D. Dietrich, R. Enami, A. Feliciello, C. Ferguson, H. Fesefeldt, G. Folger, F. Foppiano, A. Forti, S. Garelli, S. Giani, R. Giannitrapani, D. Gibin, J.G. Cadenas, I. González, G.G. Abril, G. Greeniaus, W. Greiner, V. Grichine, A. Grossheim, S. Guatelli, P. Gumplinger, R. Hamatsu, K. Hashimoto, H. Hasui, A. Heikkinen, A. Howard, V. Ivanchenko, A. Johnson, F. Jones, J. Kallenbach, N. Kanaya, M. Kawabata, Y. Kawabata, M. Kawaguti, S. Kelner, P. Kent, A. Kimura, T. Kodama, R. Kokoulin, M. Kossov, H. Kurashige, E. Lamanna, T. Lampén, V. Lara, V. Lefebure, F. Lei, M. Liendl, W. Lockman, F. Longo, S. Magni, M. Maire, E. Medernach, K. Minamimoto, P.M.

de Freitas, Y. Morita, K. Murakami, M. Nagamatu, R. Nartallo, P. Nieminen, T. Nishimura, K. Ohtsubo, M. Okamura, S. O'Neale, Y. Oohata, K. Paech, J. Perl, A. Pfeiffer, M. Pia, F. Ranjard, A. Rybin, S. Sadilov, E.D. Salvo, G. Santin, T. Sasaki, N. Savvas, Y. Sawada, S. Scherer, S. Sei, V. Sirotenko, D. Smith, N. Starkov, H. Stoecker, J. Sulkimo, M. Takahata, S. Tanaka, E. Tcherniaev, E.S. Tehrani, M. Tropeano, P. Truscott, H. Uno, L. Urban, P. Urban, M. Verderi, A. Walkden, W. Wander, H. Weber, J. Wellisch, T. Wenaus, D. Williams, D. Wright, T. Yamada, H. Yoshida, D. Zschiesche, Geant4—a simulation toolkit, Nucl. Instrum. Methods Phys. Res. A 506 (3) (2003) 250–303, http://dx.doi.org/10.1016/s0168-9002(03)01368-8.

[31] V. Ivanchenko, Geant4: physics potential for HEP instrumentation, Nucl. Instrum. Methods Phys. Res. A 494 (1–3) (2002) 514–519, http://dx.doi.org/10.1016/s0168-9002(02)01542-5.

[32] S. Meylan, U. Vimont, S. Incerti, I. Clairand, C. Villagrasa, Geant4-DNA simulations using complex DNA geometries generated by the DnaFabric tool, Comput. Phys. Comm. 204 (2016) 159–169, http://dx.doi.org/10.1016/j.cpc.2016.02.019.

[33] H. Tran, A. Marchix, A. Letourneau, J. Darpentigny, A. Menelle, F. Ott, J. Schwindling, N. Chauvin, Comparison of the thermal neutron scattering treatment in MCNP6 and GEANT4 codes, Nucl. Instrum. Methods Phys. Res. A 893 (2018) 84–94, http://dx.doi.org/10.1016/j.nima.2018.02.094.

[34] V. Milano, Acquedotti – Guida Alla Progettazione, Hoepli Editore, Milano, 2012.

[35] A. D'Aniello, L. Cimorelli, D. Pianese, Leaking pipes and the urban karst: a pipe scale numerical investigation on water leaks flow paths in the subsurface, J. Hydrol. 603 (2021) 126847, http://dx.doi.org/10.1016/j.jhydrol.2021.126847.

[36] J. Berame, E.P. Elazegui, M.C. Arenas, J.A. Orozco, Microclimatic factors and soil characteristics of arroceros forest park in the City of Manila, Philippines, Biodivers. J. Biol. Divers. 22 (11) (2021) http://dx.doi.org/10.13057/biodiv/d221130.

[37] J. Jakobi, J.A. Huisman, M. Köhli, D. Rasche, H. Vereecken, H.R. Bogena, The footprint characteristics of cosmic ray thermal neutrons, Geophys. Res. Lett. 48 (15) (2021) http://dx.doi.org/10.1029/2021gl094281.

[38] X. Wang, Y. Liu, L. Liu, Z. Wei, R. Duan, H. Wang, X. Ren, Numerical analysis on liquid seepage - Diffusion coupled with heat in soil of low - pressure buried pipelines leakage, J. Clean. Prod. 406 (2023) 137157, http://dx.doi.org/10.1016/j.jclepro.2023.137157.

[39] D. Pagano, G. Bonomi, A. Donzella, A. Zenoni, G. Zumerle, N. Zurlo, EcoMug: an efficient COsmic MUon generator for cosmic-ray muon applications, Nucl. Instrum. Methods Phys. Res. A 1014 (2021) 165732.

[40] T. Sato, Analytical model for estimating terrestrial cosmic ray fluxes nearly anytime and anywhere in the world: Extension of PARMA/EXPACS, in: Q. Zhang (Ed.), PLoS One 10 (12) (2015) e0144679, http://dx.doi.org/10.1371/journal.pone.0144679.

[41] T. Sato, Analytical model for estimating the Zenith angle dependence of terrestrial cosmic ray fluxes, in: Q. Zhang (Ed.), PLoS One 11 (8) (2016) e0160390, http://dx.doi.org/10.1371/journal.pone.0160390.

[42] Z. Ge, R. Xu, H. Wu, Y. Zhang, G. Chen, Y. Jin, N. Shu, Y. Chen, X. Tao, Y. Tian, P. Liu, J. Qian, J. Wang, H. Zhang, L. Liu, X. Huang, CENDL-3.2: The new version of Chinese general purpose evaluated nuclear data library, in: Z. Ge, N. Shu, Y. Chen, W. Wang, H. Zhang (Eds.), EPJ Web Conf. 239 (2020) 09001, http://dx.doi.org/10.1051/epjconf/202023909001.

[43] M. Quinta-Ferreira, J.F. Dias, S. Alija, False low water content in road field compaction control using nuclear gauges: a case study, Environ. Earth Sci. 75 (14) (2016) http://dx.doi.org/10.1007/s12665-016-5901-1.

[44] M. Andreasen, K.H. Jensen, H. Bogena, D. Desilets, M. Zreda, M.C. Looms, Cosmic ray neutron soil moisture estimation using physically based site-specific conversion functions, Water Resour. Res. 56 (11) (2020) http://dx.doi.org/10.1029/e2019wr026588.

[45] M.J. Brandt, K.M. Johnson, A.J. Elphinston, D.D. Ratnayaka, Hydrology and surface supplies, in: Twort's Water Supply, Elsevier, 2017, pp. 65–116, http://dx.doi.org/10.1016/b978-0-08-100025-0.00003-x.

[46] M. Schrön, M. Köhli, L. Scheiffele, J. Iwema, H.R. Bogena, L. Lv, E. Martini, G. Baroni, R. Rosolem, J. Weimar, J. Mai, M. Cuntz, C. Rebmann, S.E. Oswald, P. Dietrich, U. Schmidt, S. Zacharias, Improving calibration and validation of cosmic-ray neutron sensors in the light of spatial sensitivity, Hydrol. Earth Syst. Sci. 21 (10) (2017) 5009–5030, http://dx.doi.org/10.5194/hess-21-5009-2017.

[47] D. Rasche, M. Köhli, M. Schrön, T. Blume, A. Güntner, Towards disentangling heterogeneous soil moisture patterns in cosmic-ray neutron sensor footprints, Hydrol. Earth Syst. Sci. 25 (12) (2021) 6547–6566, http://dx.doi.org/10.5194/hess-25-6547-2021.